



Rotordynamics analysis of solar hybrid microturbine for concentrated solar power

Maulana Arifin^{a, b, *}

^a Research Centre for Electrical Power and Mechatronics, Indonesian Institute of Sciences
Komp LIPI Bandung, Gd 20, Lt 2, Bandung, West Java, 40135 Indonesia

^b Institute of Thermal Turbomachinery and Machinery Laboratory, University of Stuttgart
Pfaffenwaldring 6, 70569 Stuttgart, Germany

Received 15 May 2020; accepted 18 June 2020; Published online 30 July 2020

Abstract

Microturbine based on a parabolic dish solar concentrator runs at high speed and has large amplitudes of subsynchronous turbo-shaft motion due to the direct normal irradiance (DNI) fluctuation in daily operation. A detailed rotordynamics model coupled to a full fluid film radial or journal bearing model needs to be addressed for increasing performance and to ensure safe operating conditions. The present paper delivers predictions of rotor tip displacement in the microturbine rotor assembly supported by a journal bearing under non-linear vibrations. The rotor assembly operates at 72 krpm on the design speed and delivers a 40 kW power output with the turbine inlet temperature is about 950 °C. The turbo-shaft oil temperature range is between 50 °C to 90 °C. The vibrations on the tip radial compressor and turbine were presented and evaluated in the commercial software GT-Suite environment. The microturbine rotors assembly model shows good results in predicting maximum tip displacement at the rotors with respect to the frequency and time domain.

©2020 Research Centre for Electrical Power and Mechatronics - Indonesian Institute of Sciences. This is an open access article under the CC BY-NC-SA license (<https://creativecommons.org/licenses/by-nc-sa/4.0/>).

Keywords: microturbines rotor tip displacement; parabolic dish solar concentrator; rotordynamics model; journal bearing; non-linear vibration.

I. Introduction

Concentrating solar power (CSP) is presently primary technology for generating power electricity from solar energy after Photovoltaics (PV). Commercial CSP technology can be commonly divided into the following four main types, that is, linear fresnel reflector, parabolic trough collector, central receiver, and parabolic dish [1]. CSP utilizes mirrors set to focus the direct sunlight onto a solar receiver to increase the working fluid temperature. The working fluid then converts its energy to mechanical energy in the thermal engine to produce electrical power.

In many studies, it is recognized that parabolic troughs employ reflective surface or mirror with a parabolic-shaped cross-section, which delivers a linear concentration on the receiver tube where a heat transfer fluid temperature can be increased up to 390 °C. The parabolic troughs concentration ratio

is typically below 80 [2]. Comparable to parabolic troughs, linear Fresnel reflector (LFR) systems can heat the working fluid to 450 °C and are generally used in power plants of a few megawatts. Meanwhile, central solar towers and parabolic dish solar concentrators have a higher concentration ratio than a parabolic trough (typically more than 1000). Both of them have the potential to raise the working fluid to 800 °C, which is necessary for certain types of thermal engines such as gas turbines. However, the solar towers are not applicable for small scale power generation applications (< 50 kW). Therefore, a parabolic dish solar concentrator becomes the most suitable for such applications [3].

In the parabolic dish solar concentrator system, microturbine is a crucial component to increase its power and performance. The microturbine consists of turbomachinery components such as radial compressors and turbines [4]. Due to the light and small rotor dimensions, microturbine runs at high rotor speeds in various operating conditions. Typical rotor speed is around 50,000 to 150,000 rpm, which delivers mechanical or structural stability issues. Poor design of the microturbine components can

* Corresponding Author. Tel: +49-711-685-63516
E-mail address: maulana.arifin@lpi.go.id

cause low performance and even failure in the assembly system. To overcome these critical issues, a rotordynamic analysis in compressors and turbines can be very beneficial for ensuring safety and increasing the system performance [5]. The non-linear vibration on the journal or thrust bearing and turboshaft of turbocharger compressor and turbine have been extensively studied in the open literature [6][7]. Researchers attempted to evaluate the impact of mode shape degeneration in linear rotordynamics and the effect of thrust bearing for turbocharger components [8][9]. However, rotordynamics analysis on the microturbine based on CSP application did not obtain much attention in the open literature and nearly a few works have been presented [5]. The present study highlights a non-linear rotordynamics analysis at design and off-design on the rotor speed of microturbine for CSP applications. This could be useful for readers in determining a suitable rotor design, especially for high-speed microturbine applications. This paper also aims to gain more insights into the effect of journal bearing clearance at the turbo-shaft of microturbine.

II. Materials and Methods

In the present study, the turbomachinery components are using cast aluminium material for the radial compressor and Inconel-718 for the radial turbine. Table 1 shows performance data for both the radial compressor and the turbine components. The power output of the system is about 40 kW at the design point with the turbine inlet temperature (TIT) of 950 °C. The weights of the rotors are 100 and 150 grams. For the mechanical supports, the

turbo-shaft uses a journal bearing with inner and outer bushing. The primary function of a journal bearing is to maintain the wheels or rotors balance (rotordynamics stability) at all operating conditions of microturbine. Due to an interaction between joints and force elements, the rotor assembly modelling is based on the multibody dynamics structure [10]. The turbo-shaft rotor is defined as an assembly of rigid and flexible bodies. Therefore, the existing hydrodynamic bearings restrict the global motion in an axial and radial direction (see Figure 1). A sleeve bearing is fit into radial compressor journal bearing end and seal installation from the lubricant oil 5W30-62. The oil temperature at the operating condition is between 50 °C to 90 °C.

The Reynolds lubrication equation is utilized to calculate the flow dynamics and bearing forces in the oil film journal bearing [11]. The numbers for oil film at journal bearing are typically laminar between 100 and 200. The Reynolds lubrication equation can be written as:

$$\frac{\partial}{\partial x} \left(h^3 \frac{\partial p}{\partial x} \right) + \frac{\partial}{\partial z} \left(h^3 \frac{\partial p}{\partial z} \right) = 6\eta \left[(U_j + U_b) \frac{\partial h}{\partial x} + 2 \frac{\partial h}{\partial t} \right] \quad (1)$$

where U_j is the journal velocity; U_b is the bearing ring velocity; h is the oil film thickness; x is the circumferential direction ($x = R$); z is the axial direction. Based on Nguyen-Schäfer [11], the non-linear bearing force is defined as:

$$F_1 = +F_r \sin \gamma + F_t \cos \gamma \equiv f_1(\varepsilon, \dot{\varepsilon}, \gamma, \dot{\gamma}, \Omega) \quad (2)$$

$$F_2 = -F_r \cos \gamma + F_t \sin \gamma \equiv f_2(\varepsilon, \dot{\varepsilon}, \gamma, \dot{\gamma}, \Omega) \quad (3)$$

where F_1 and F_2 are pressure force components at inertial coordinates; F_r and F_t are the bearing forces in the rotating coordinate system (r, t); Ω is the

Table 1. Table caption data specification of the radial compressor and radial turbine at the design point

Parameter	Unit	Compressor	Turbine
Mass flow rate (\dot{m})	[kg/s]	0.34	0.34
Rotor speed (Ω)	[rpm]	72,373	72,373
Power (P)	[kW]	40	80
Efficiency (η_{ts})	[-]	0.78	0.84
Pressure Ratio (PR)	[-]	2.8	2.6
Turbine Inlet Temperature	[K]	-	1,173
Number of blade rotor (Z_r)	[-]	8/8	16
Number of blade vane (Z_v)	[-]	-	17
Diameter rotor	[mm]	105	128
Axial length	[mm]	41	42
High of rotor outlet (B2)	[mm]	6.8	25
Beta angle (Beta2B)	[°]	-40	-

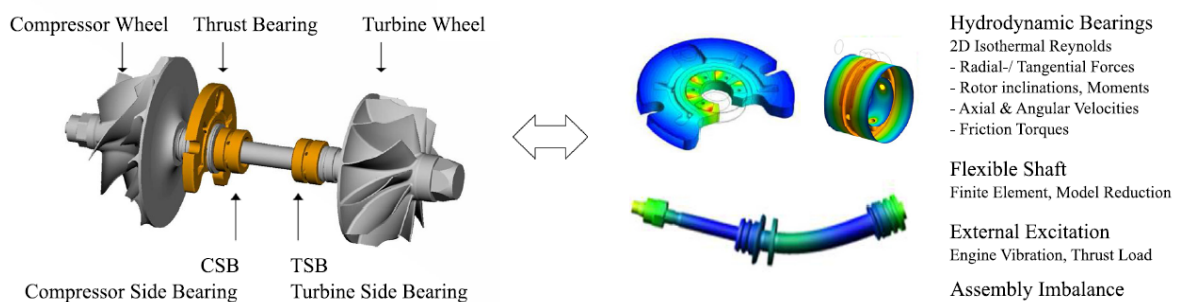


Figure 1. Radial compressor and turbine assembly modeling with turbo-shaft and bearing [10]

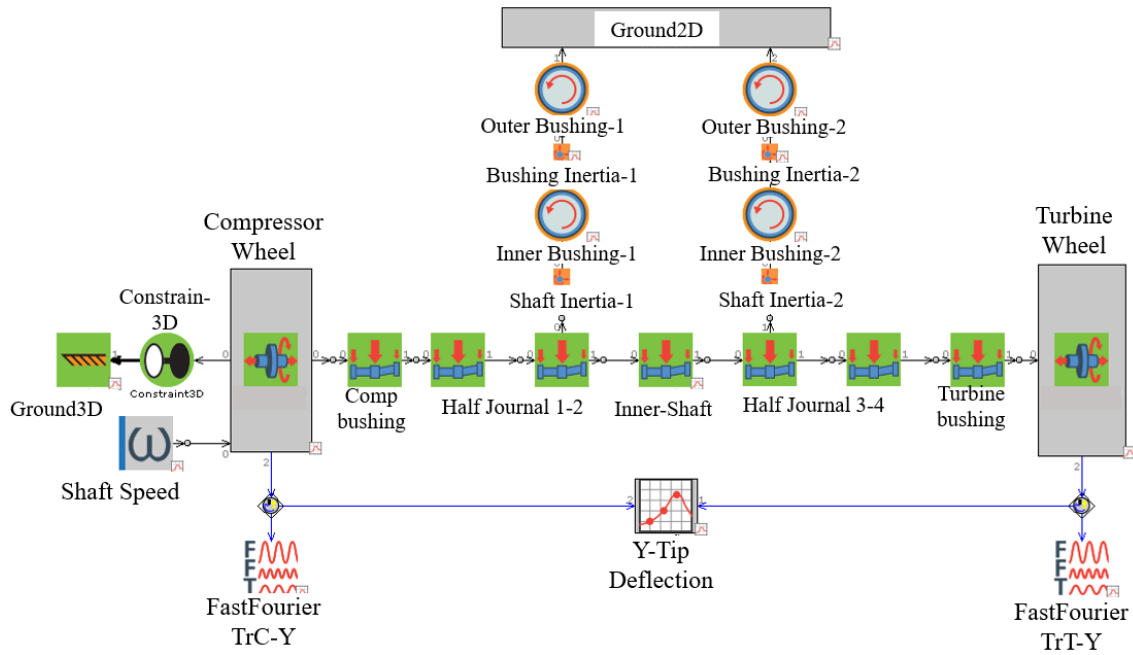


Figure 2. Radial compressor and turbine assembly modeling with turbo-shaft and bearing

angular rotor velocity or rotor speed; ε and $\dot{\varepsilon}$ are the journal bearing relative eccentricity and the time change rate of the journal relative eccentricity; γ is the whirl velocity of the journal bearing. The equation above is utilized to calculate the transient non-linear bearing forces at every iteration time step. The solutions are from the damping coefficients, bearing stiffness, and other parameters [11]. The bearing stiffness coefficients k_{ik} on Equation (4) and the bearing damping coefficients d_{ik} on Equation (5) are defined from the static load (F_0), radial bearing clearance (c), journal bearing dimensionless damping coefficients (β_{ik}), and the rotor speed:

$$k_{ik} \equiv -\frac{\partial f_i}{\partial x_k} = \kappa_{ik} \frac{F_0}{c}; \quad i; k = 1, 2 \quad (4)$$

$$d_{ik} \equiv -\frac{\partial f_i}{\partial \dot{x}_k} = \beta_{ik} \frac{F_0}{c\Omega}; \quad i; k = 1, 2 \quad (5)$$

In the present study, the rotordynamics in microturbine as mentioned above were developed and solved in the commercial tool GT-Suite environment [12]. In GT-Suite, the characteristics of turbo-shaft and rotor vibrations are defined in the frequency and time domain. In the frequency domain, the harmonic vibration has the same frequency of the rotor frequency Ω . The frequency order is called 1X which is $\omega = \Omega$ [11][13].

Meanwhile, in the time domain, the harmonic vibration has a time function of sine or cosine or $x(t) = A \sin(\Omega t + \varphi)$, where $x(t)$ is the time amplitude of the vibration and φ is the phase in radian. Figure 2 shows the microturbine rotor assembly model implemented in GT-Suite environment to compute the rotordynamics phenomena and the effect of the journal bearing clearance.

III. Results and Discussions

A. Rotordynamics of rotor assembly on the design and off-design speed

In this section, the rotordynamics simulations on the microturbine turbo-shaft with journal bearing and inner-outer bushing support are presented. The turbo-shaft runs at design speed 72 krpm and compared to the off-design speed operating conditions. Figure 3 shows the dependency of the results upon the Fast Fourier Transform (FFT) on the input signal concerning the time domain for both compressor and turbine. The input signal FFT represents superimposed vibration in the Y-direction and the vibration response to the rotors [11]. It can be seen that in the turbine, the vibration is higher than in the compressor wheel.

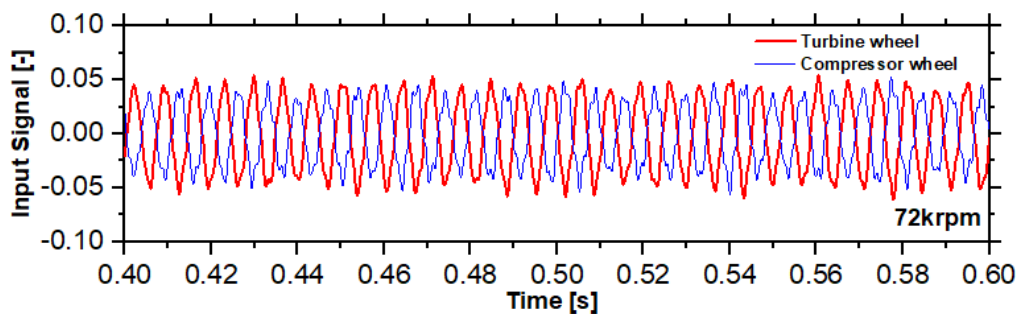


Figure 3. The Fast Fourier Transform (FFT) on the input signal vs. time domain for compressor and turbine

Figure 4 presents the influence of rotor speed on the tip displacements at the compressor and turbine concerning the time domain. The tip deflection or displacements on the rotor is in the Y-direction with the transient response. Five different speeds are considered, i.e. 52 krpm, 57 krpm, 65 krpm, 72 krpm (design speed), and 79 krpm. These represent 0.7 to 1.1 of the design speed. For the rotor speed of 52 krpm and 57 krpm (Figures 4A and 4B), the tip deflection characteristics are similar. It can be seen that the rotor tip deflection or displacement is unstable at the beginning. The vibration starts at the initial position and grows exponentially with time, hence the vibration becomes unstable. The

behaviour of vibration becomes stable after several times due to the decrease in the amplitude of the vibration in a short time (see Figure 5). For instance, the maximum tip displacement at the stable region for both compressor and turbine are below 0.02 mm. Figures 4B, 4C, and 4D reveal that there has been a gradual increase in the maximum tip displacement for compressor and turbine. The vibration characteristics of the rotors are similar from rotor speed 65 krpm to 79 krpm (Figures 4C and 4D). The maximum tip displacement is between 0.05 mm to 0.07 mm, which is still at the safe operating conditions [14].

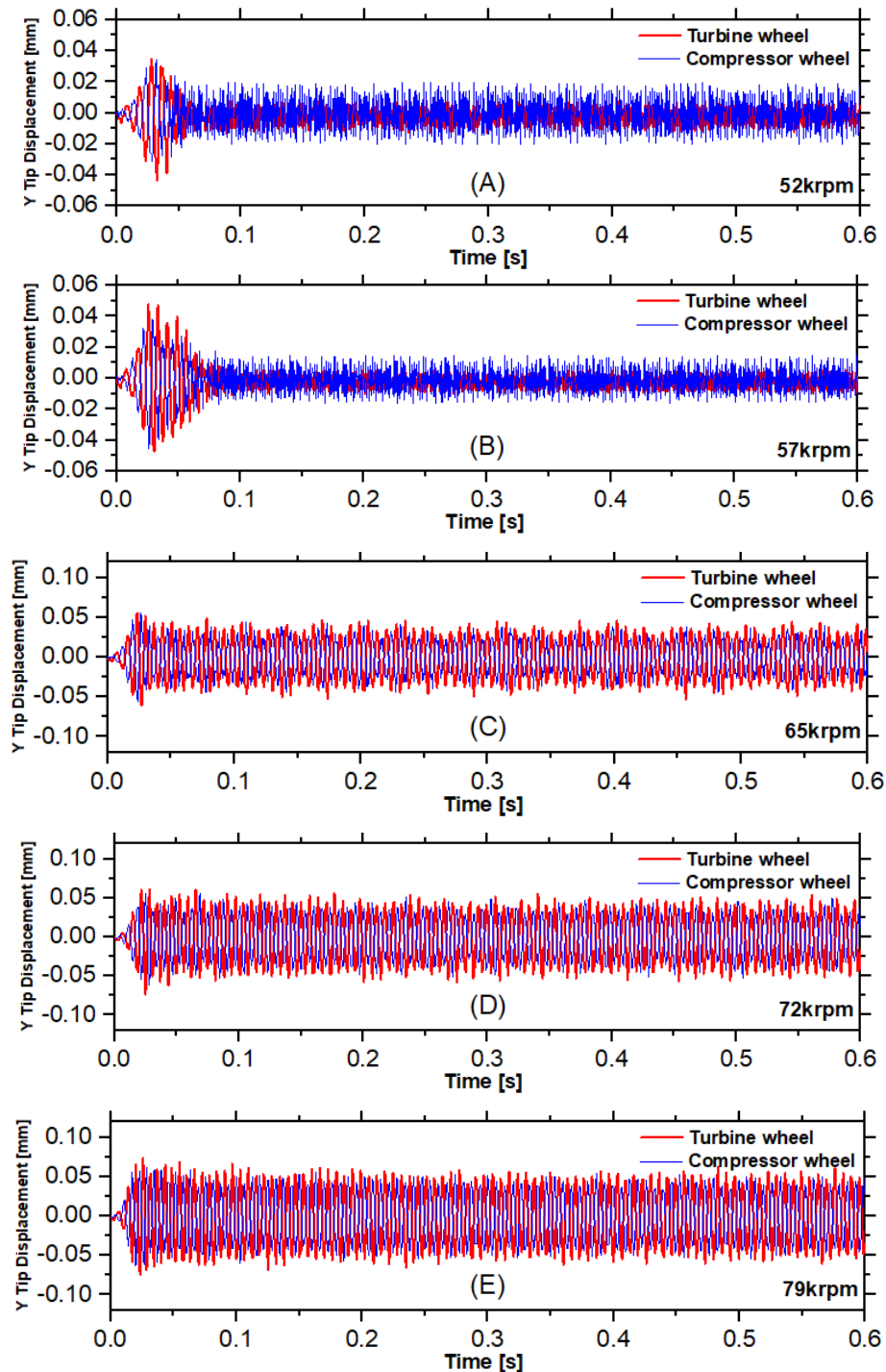


Figure 4. Prediction of the maximum tip displacement for compressor and turbine wheel at various turbo speed: (A) 52 krpm; (B) 57 krpm; (C) 65 krpm; (D) 72 krpm; (E) 79 krpm

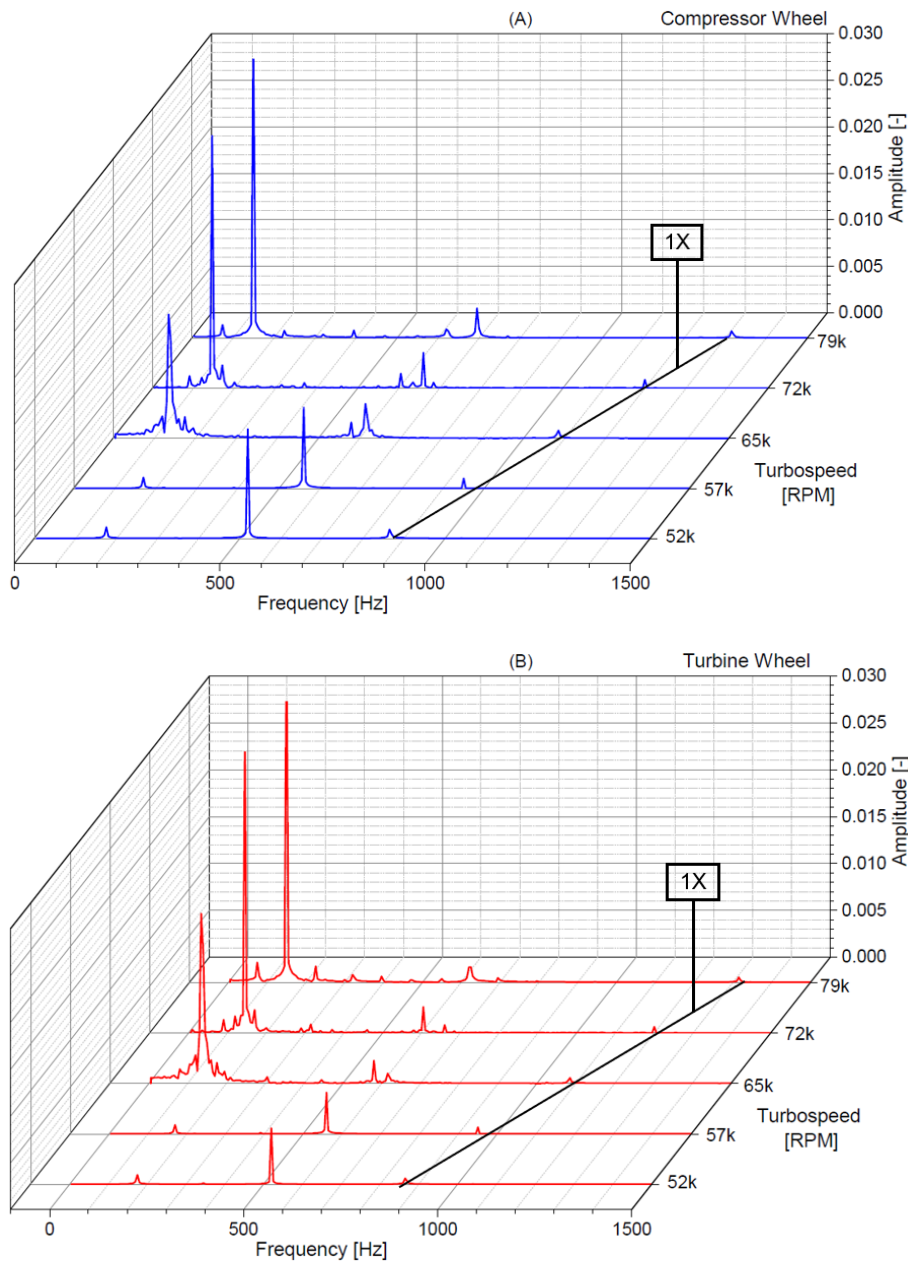


Figure 5. The non-linear rotordynamics prediction of the maximum amplitude for (A) compressor and (B) turbine wheel at various turbo speed in the frequency domain

Figure 5 depicts a waterfall diagram of predicted non-linear turbo-shaft response at compressor and turbine. The waterfall diagram in Figures 5A and 5B also expose the rotor mode shapes at a turbo-shaft from 52 krpm to 79 krpm. In most cases, the journal bearing system critical speeds are recognized on the crossing of the synchronous line 1X ($\omega = \Omega$) with each of the natural frequencies. For safety reasons, the design of journal bearing should avoid crossing the natural frequencies line. Figures 5A and 5B show that the unbalance amplitude at synchronous line 1X is relatively small, which means that the journal bearing or turbo-shaft of the compressor and turbine wheel are running safely. Meanwhile, the frequency of the journal bearing is much higher than the quasi-resonance amplitude of the compressor and turbine wheel. The maximum amplitude is about 0.030 and 1300 Hz for the maximum frequency. The characteristic resonance of linear vibration does not

present in non-linear rotordynamics simulation [14]. Therefore, only the maximum cycle of the compressor and turbine wheel response is developed at each turbo speed.

B. Effect of the journal bearing clearance

The influence of the oil journal bearing clearance is discussed in this section. The turbo-shaft operates at the design speed of 72 krpm. Five difference clearances are considered, that is 0.015 mm, 0.020 mm, 0.025 mm, 0.030 mm, and 0.035 mm. Figure 6 displays the comparison of maximum tip displacement for both compressor and turbine wheel. Similar to the previous section, the tip displacement of the rotor response is obtained through superimposing the harmonic unbalance vibration on the subsynchronous frequency components of the inner and outer oil journal bearing at the rotor. For the oil journal bearing

clearance of 0.015 mm, the tip displacement increases and becomes unbalanced at the beginning time step simulation. The maximum displacement is about 0.04 mm (see Figure 6A). Furthermore, Figure 6B shows that the vibration of the rotor response has

sidebands displacement at the initial time step. In the end, the vibration response is diminished with the minimum displacement. However, the tip displacement trend is increased at the more significant journal bearing clearance, as shown in

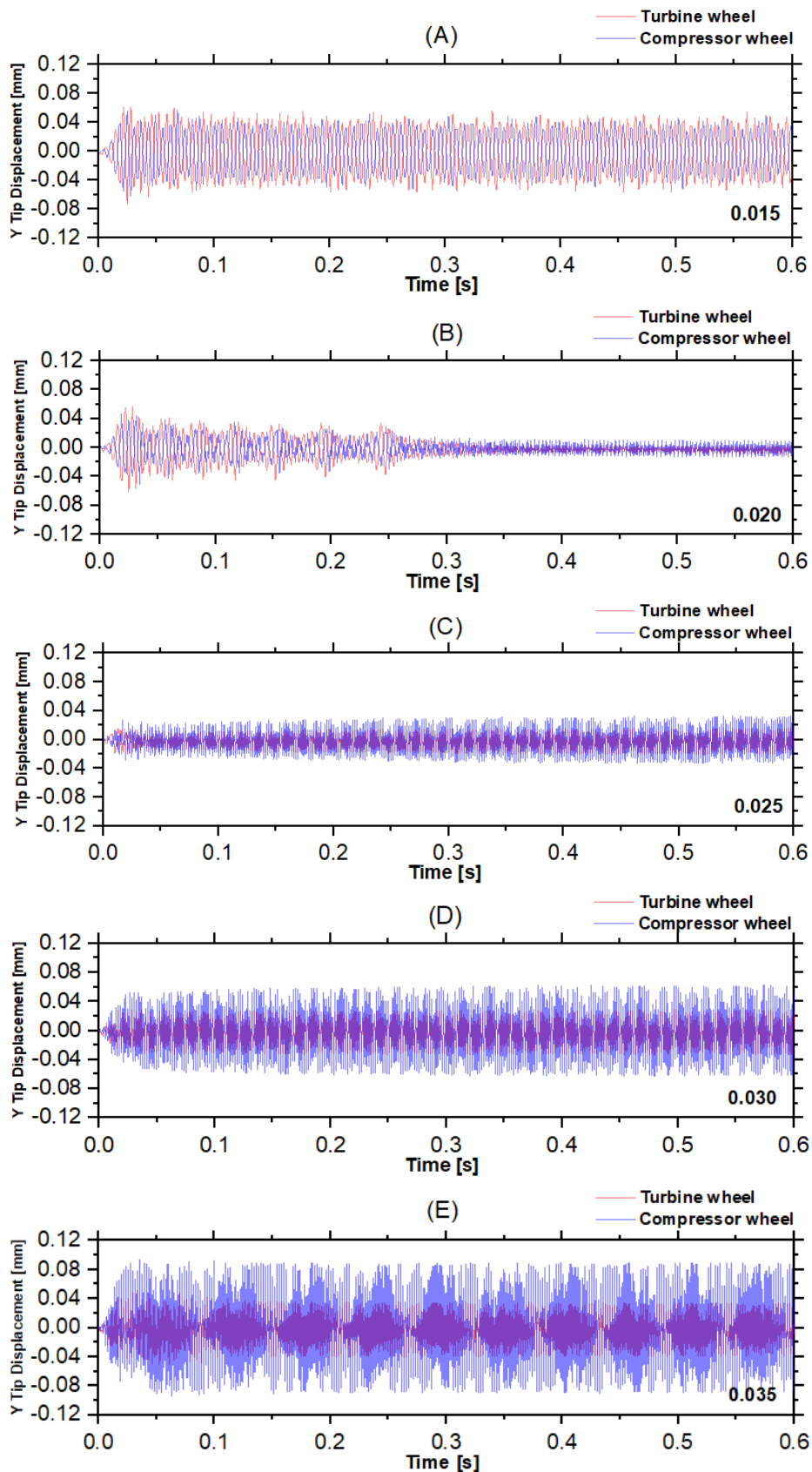


Figure 6. Comparison of maximum tip displacement at different journal bearing clearance for compressor and turbine wheel: (A) 0.015; (B) 0.020; (C) 0.025; (D) 0.030; (E) 0.035

Figures 6C, 6D, and 6E. At the 0.035 mm clearance, the maximum displacement is about 0.09 mm. From Figure 6 it is known that the ideal clearances for turbo-shaft microturbine are between 0.015 mm and 0.020 mm at the design point operation. To conclude, the turbomachinery components for CSP system require a wider range of rotational speed and loading than conventional micro gas-turbine to maintain high efficiency due to fluctuation in DNI daily operation [15].

IV. Conclusion

The rotordynamics characteristics of turbo-shaft microturbine based on parabolic dish solar concentrator were investigated under non-linear vibrations in the time and frequency domains. The model can predict a maximum tip displacement for compressor and turbine wheel at various speed. Five different turbo speed values and journal bearing oil clearance were considered in the evaluations. This study used a Fast Fourier Transform (FFT) to represent the vibrations response to the rotor or wheel. This study shows that the maximum tip displacement occurs at higher turbo speed and larger bearing oil clearance. The results show that in the design turbo speed (72 krpm), the maximum tip displacement is still in reasonable conditions.

Acknowledgement

The authors would like to acknowledge the Ministry of Finance Republic of Indonesia for the financial support through Indonesia Endowment Fund for Education (LPDP), Insentif Riset Sistem Inovasi Nasional (INSINAS) Kemenristek, and the Institute of Thermal Turbomachinery and Machinery Laboratory (ITSM) at the University of Stuttgart for providing the computational support.

Declarations

Author contribution

M. Arifin as the contributor of this paper. Author read and approved the final paper.

Funding statement

This research did not receive any specific grant from funding agencies in the public, commercial, or not-for-profit sectors.

Conflict of interest

The authors declare no conflict of interest.

Additional information

No additional information is available for this paper.

References

- [1] M.D.J.M. Guerrero-Lemus R., "Concentrated Solar Power," in: *Renewable Energies and CO₂*, Vol. 3. London: Springer-Verlag, 2013.
- [2] W.S.K. Lovegrove, *Concentrating Solar Power Technology, Principles, Developments and Applications*, Woodhead Publishing, 2012.
- [3] M. Arifin, A. Rajani, Kusnadi, and T. D. Atmaja, "Modeling and Performance Analysis of a Parallel Solar Hybrid Micro Gas Turbine," *Proceeding - 2019 Int. Conf. Sustain. Energy Eng. Appl. Innov. Technol. Towar. Energy Resilience, ICSEEA 2019*, pp. 62–68, 2019.
- [4] M. Arifin, K. Kusnadi, and R. I. Pramana, "Prediction performance map of radial compressor for system simulation," *Proc. - 6th Int. Conf. Sustain. Energy Eng. Appl. ICSEEA 2018*, pp. 51–56, 2019.
- [5] A.I.S.A. Arroyo, M. McLorn, M. Fabian, M. White, "Rotor-Dynamics of Different Shaft Configurations for a 6 kW Micro Gas Turbine for Concentrated Solar Power," *ASME Turbo Expo 2016 Turbomach. Tech. Conf. Expo.*, pp. 1–10, 2016.
- [6] I. Chatzisavvas, "Efficient Thermohydrodynamic Radial and Thrust Bearing Modeling for Transient Rotor Simulations," *PhD Thesis, Darmstadt, Tech. Univ.*, 2018.
- [7] M.I. Friswell, *Dynamics of Rotating Machines*. Cambridge University Press, 2015.
- [8] P. Koutsovasilis, "Mode shape degeneration in linear rotor dynamics for turbocharger systems," *Arch. Appl. Mech.*, vol. 87, no. 3, pp. 575–592, 2017.
- [9] I. Chatzisavvas, "Efficient Thrust Bearing Model for High-Speed Rotordynamic Applications," in *Proceedings of the 9th IFToMM International Conference on Rotor Dynamics*, 2015.
- [10] P. Koutsovasilis, "Automotive turbocharger rotordynamics: Interaction of thrust and radial bearings in shaft motion simulation," *J. Sound Vib.*, vol. 455, pp. 413–429, 2019.
- [11] H. Nguyen-Schäfer, *Rotordynamics of Automotive Turbochargers*, vol. 2. Stuttgart: Springer International Publishing AG Switzerland, 2015.
- [12] Gamma Technologies, "GT-Suite, Flow and Mechanical Theory Manual," 2019.
- [13] C.U. Waldherr and D.M. Vogt, "An Extension of the Classical Subset of Nominal Modes Method for the Model Order Reduction of Gyroscopic Systems," *J. Eng. Gas Turbines Power*, vol. 141, no. 5, pp. 1–8, 2019.
- [14] W.J. Chen, "Rotordynamics and bearing design of turbochargers," *Mech. Syst. Signal Process.*, vol. 29, pp. 77–89, 2012.
- [15] D. Iaria, J. Alzaili, A.I. Sayma, "Solar Dish Micro Gas Turbine Technology for Distributed Power Generation," In *Sustainable Energy Technology and Policies. Green Energy and Technology*, Springer, Singapore, 2018.